# Accepted Manuscript

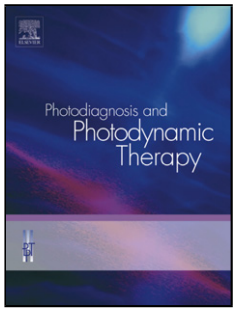


Title: Photothermally enhanced bactericidal activity by the combined effect of NIR laser and unmodified graphene oxide against *Pseudomonas aeruginosa*

Authors: Jésica Yanina Pereyra, Emma Antonia Cuello, Horacio Javier Salavagione, César Alfredo Barbero, Diego Fernando Acevedo, Edith Inés Yslas

PII: S1572-1000(18)30129-7
DOI: https://doi.org/10.1016/j.pdpdt.2018.08.018
Reference: PDPDT 1238

To appear in: *Photodiagnosis and Photodynamic Therapy*

Received date: 25-4-2018
Revised date: 15-8-2018
Accepted date: 27-8-2018

Please cite this article as: Pereyra JY, Cuello EA, Salavagione HJ, Barbero CA, Acevedo DF, Yslas EI, Photothermally enhanced bactericidal activity by the combined effect of NIR laser and unmodified graphene oxide against *Pseudomonas aeruginosa*, *Photodiagnosis and Photodynamic Therapy* (2018), https://doi.org/10.1016/j.pdpdt.2018.08.018

# Photothermally enhanced bactericidal activity by the combined effect of NIR laser and unmodified graphene oxide against *Pseudomonas aeruginosa*.

Jésica Yanina Pereyra[a], Emma Antonia Cuello[a], Horacio Javier Salavagione[b], César Alfredo Barbero[a*], Diego Fernando Acevedo[a,c], and Edith Inés Yslas[a,d]*.

[a] Instituto de Investigaciones en Tecnologías Energéticas y Materiales Avanzados (IITEMA), Universidad Nacional de Río Cuarto (UNRC)-Consejo Nacional de Investigaciones Científicas y Técnicas (CONICET) Ruta 8 y 36 Km 601, X5804ZAB, Río Cuarto (Córdoba), Argentina.

[b] Departamento de Física de Polímeros, Elastómeros y Aplicaciones Energéticas, Instituto de Ciencia y Tecnología de Polímeros (ICTP-CSIC), Juan de la Cierva 3, 28006 Madrid, Spain.

[c] Departamento de Tecnología Química. Facultad de Ingeniería, Universidad Nacional de Río Cuarto, Ruta 36 Km 601, 5800, Río Cuarto, Argentina

[d] Departamento de Biología Molecular, CONICET, Facultad de Ciencias Exactas, Fisicoquímicas y Naturales, Universidad Nacional de Río Cuarto, Ruta 36 Km 601, 5800, Río Cuarto, Argentina

*Corresponding authors
Dra. Edith I. Yslas, email: eyslas@exa.unrc.edu.ar
Dr. Cesar Barbero, email: cbarbero@exa.unrc.edu.ar

## Graphical abstract

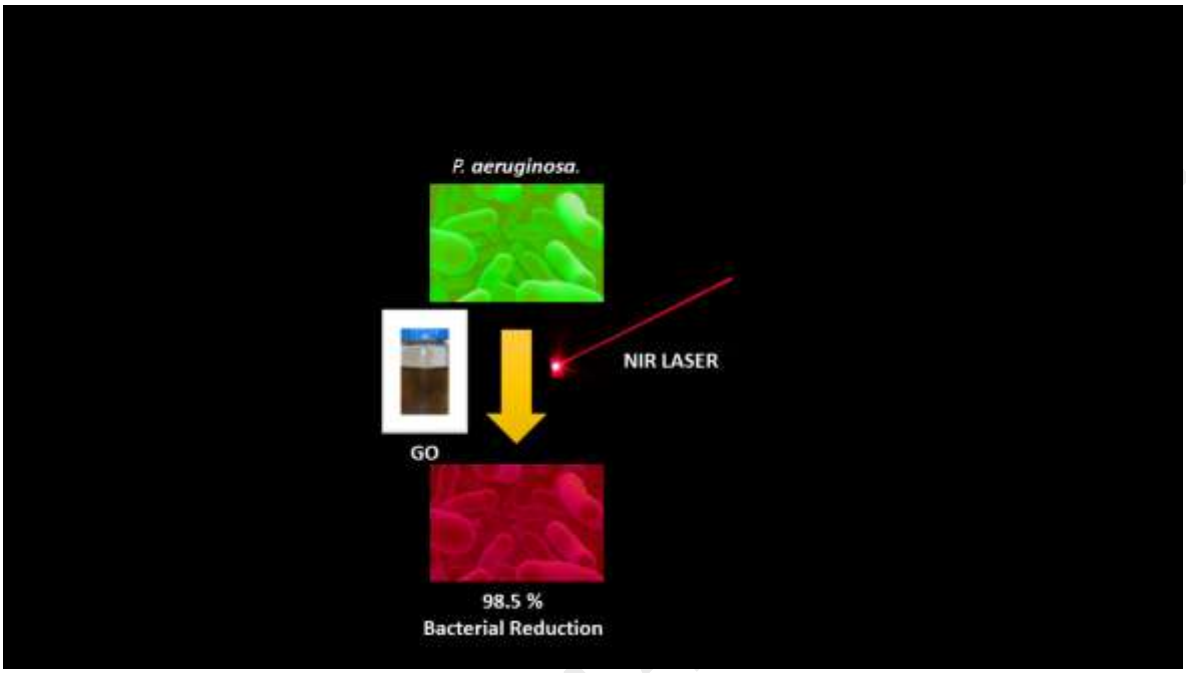


## Highlights

- A novel therapy for combating bacteria avoiding the use of antibiotics is shown
- GO dispersions (120 μg/mL) exhibit antibacterial performance against *P. aeruginosa*
- GO dispersions (>2 μg/mL) kill *P. aeruginosa* only under NIR irradiation
- A 98.49 % killing rate is achieved (5 min NIR irradiation and 2 μg/mL of GO)
- GO may be utilized as localized photothermal agent
- GO could be used for clinical treatment of bacterial infections of soft tissues.

## Abstract

The manuscript shows the application of unmodified graphene oxide (GO) as a photothermally susceptible material to trigger antibacterial effects. The synthesis and characterization of unmodified GO easily dispersed in aqueous solutions is also shown. High

GO concentrations in the dark and low GO concentrations irradiated with near infrared light (NIR) produced death in nosocomial bacterium (*Pseudomonas aeruginosa*). It is demonstrated that GO dispersion in the dark produced a dose-dependent increase in the antibacterial action at concentrations up to 120 µg/mL. On the other hand, by using much lower concentrations (c.a. 2 µg/mL) of GO (non toxic in the dark) and irradiating with near-infrared radiation during 15 min, a degree of mortality of 98.49 % was observed. The *P. aeruginosa* treated with GO and irradiated exhibited DNA fragmentation due to the physical damage of cell membranes. The GO 2 µg/mL dispersions proved favorable, since they do not induce cell death in the dark, whereas the combination with NIR light triggers the damage to the cell membranes. This characteristic is clearly an advantage in comparison with traditional antibacterial nanomaterials (such as nanoparticles), which induce cell killing due to the nanoparticles toxicity *per se*. Furthermore, this work provides a novel treatment for combating bacterial nosocomial infections without the use of antibiotics, opening a new area of clinical application via simple photothermal therapy.

**Keywords:** Photothermal therapy; graphene oxide; antibacterial activity; near infrared; *Pseudomonas aeruginosa*

## 1. Introduction

Bacteria are microorganisms that can cause deadly infections. In immunocompromised individuals, *Pseudomonas aeruginosa* is a common nosocomial pathogen causing serious infections associated with a high rate of morbidity and mortality [1]. Additionally, pathogenic

bacteria have evolved and showed great resistance against most of the conventional drugs therapies available in the market [2,3]. According to the World Health Organization, infections caused by bacteria which can resist to antibiotics is a top threat to human health [4]. Due to increased and irrational use of wide-spectrum antibiotics, the evolution and spread of antibiotic resistant bacteria is becoming a major global health threat [5]. Therefore, the development of innovative therapeutic strategies and novel antimicrobials for killing bacteria and to combat infections is becoming crucial [6].

Recent advances in nanotechnology have produced new nanomaterials that can be used to combat infectious diseases [7,8]. Moreover, during the last few years, several nanomaterials have been investigated in order to address the issue of antibiotic resistant bacteria [9]. Thus, not only new materials but also new methodologies are necessary to reverse the antibiotic resistance of pathogenic bacteria. The use of nanomaterials in photothermal processes for selective treatment of bacterial infections is a novel, recent and promising therapeutic modality [10]. Photothermal therapy (PTT) is an alternative approach in which photothermal agents are employed to produce localized heating [11]. This materials have the capacity of absorbing near-infrared light (NIR) in the spectral region where water and hemoglobin present minimal optical absorption (700 to 900 nm), that ensures maximum light penetration depth without tissue damage [12]. Various nanomaterials such as carbon nanotubes, graphene, and gold nanorods have been employed to generate sufficient heat to kill bacteria upon exposure to NIR light [13,14]. Several investigations have demonstrated that gold nanoparticles can be used as an agent in photothermal therapy to trigger the destruction of bacteria [15,16]. If the nanoparticles are attached to bacterial cells, the localized heating that occurs during NIR irradiation causes irreparable cellular damage.

Nowadays, graphene has attracted the attention of the entire scientific community because of its remarkable electrochemical, mechanical, electronic and thermal properties, which make it a potential candidate for bio-applications [17,18]. However, due to its low water solubility, many graphene derivatives have been proposed for applications where the nanomaterial structural quality is not an important issue [19]. Taking this into account, GO prepared by oxidation of graphite consists of single-atom-thick graphene layers bearing hydroxyl, epoxide, and carboxylic acid groups [20]. This material is of great interest due to its low cost, easy access, high dispersibility in water and its interesting electrical, thermal, mechanical, and optical properties [21]. The potential applications of GO are those related to biomedicine, including drug delivery, antibacterial action, biosensing and photothermal therapy, among others [22–24]. In fact, graphene nanosheets in the form of graphene nanowalls deposited on stainless steel and reduced graphene (rGO) nanosheets have already shown high potential as antibacterial agents [25]. Moreover, GO decorated with silver nanoparticles have displayed excellent antibacterial activity against *P. aeruginosa* [26]. However, to date there are no studies dealing with the effect of the GO concentration on bacterial mortality.

Several research works showed that the graphene oxide was initially considered as a biocompatible nanomaterial [27–30]. However, in *vitro* and in *vivo* toxicity studies of GO have reported contradictory results since the toxicity of GO depends on different factors such as line cell, concentration, size and synthetic methods employed [31–33]. It has been recently reported that GO with different sizes (ranging from 150 nm to 1000 nm large GO) presents a similar toxicity at low concentrations (10 μg/mL), however at concentration of 100 μg/mL the difference in toxicity as a response to size becomes obvious [34]. While the toxicity does not depend on the particle size for the RAW 264.7, NB4 and HL60 cell lines, a clear relationship between the size and cytotoxicity was observed for three adherent cell lines: NIH

3T3, A459 and U87 [34]. Another interesting study proposed that GO with particle of microns induce more severe inflammatory response than nanometric particles [35]. Chng and Pumera proposed that the cytotoxicity of GO depends on the synthetic procedure used to prepare GO [36]. Besides, the evaluation of the toxicity of GO *in vivo*, Zhang *et al.* did not find significant pathological changes in all the examined organs when mice were exposed to GO (dose 1mg/kg) for 14 days [37].

Thus, in this work the antibacterial effect of different concentrations of GO dispersions on *P. aeruginosa* is studied. Also, recent studies showed that functionalized GO and rGO have been used in photothermal therapy [38], as photothermal absorbers to kill bacteria [39]. While rGO presents higher light absorption than GO, it is insoluble in biological media since it lacks enough hydrophilic functional groups, found mainly only at edges and defects [40]. To overcome this situation, rGO was modified by adsorption of hydrophilic polymers, or with magnetic or metallic nanoparticles [38,41]. In contrast, in this work the efficiency of unmodified graphene oxide as photothermal susceptor to kill a bacteria (*P. aeruginosa*) is demonstrated, since GO contains reactive groups which are biologically more active than rGO [42]. The ability of the GO in the dispersions to act as a photothermal absorber of NIR irradiation was evaluated *in vitro*. Based on the results, it is shown that unmodified GO may be utilized as a photothermal receptor agent for NIR light against bacterial infections usually found in nosocomial situations. Therefore, a novel way to fight antimicrobial resistance in nosocomial settings avoiding the use of conventional drugs is described.

## 2. Experiments

### 2.1. Synthesis of graphene oxide

Natural graphite powder (Aldrich) was oxidized using the modified Hummers method [43]. Briefly, graphite powder (2 g) was added to concentrated $H_2SO_4$ (200 ml) immersed in an ice bath. Then, $KMnO_4$ (12 g) was added gradually under constant stirring and cooling to keep the suspension temperature below 20 °C, and the reaction left under stirring for 2 h. Subsequently, 360 ml of distilled water were added ensuring that the temperature does not exceed 50 °C. Then, 40 ml of $H_2O_2$ (a volume fraction of 30 %) was added to the mixture which adopted a bright yellow color. The mixture was washed with distilled water until the pH of the suspension reached a value of 3. The supernatant was discarded by centrifugation (30 min; 7,000 r.p.m.) and the graphite oxide dispersion obtained was dissolved in distilled $H_2O$ and subjected to ultrasound for 1 h to generate GO sheets or monolayers.

**2.2. Characterization of GO**

Fourier transform infrared (FTIR) spectra of the GO were recorded from KBr pellets of solid samples in a Nicolet Impact 410 spectrometer. The UV–Vis spectra of GO water dispersion were recorded on a HP 8452A spectrophotometer. Confocal Raman measurements were undertaken in the Raman Microspectroscopy Laboratory of the Characterization Service in the Institute of Polymer Science & Technology, CSIC using a Renishaw InVia Reflex Raman system (Renishaw plc., Wotton-under- Edge, UK), employing a grating spectrometer with a Peltier-cooled charge-coupled device (CCD) detector coupled to a confocal microscope. All spectra were processed using RenishawWiRE 3.2 software. The Raman scattering was excited using an Argon ion laser wavelength of 514.5 nm and the laser beam was focused on the sample with a 100x microscope objective (N.A. = 0.85), with a laser power at the sample of 62 mW. The average size of the GO was evaluated by High-resolution transmission

electron microscope (HRTEM) at the Centro Nacional de Microscopía Electrónica, Madrid, Spain. For measurement of GO flake lateral dimensions, HRTEM micrographs were performed on a JEOL JEM-2100 instrument, using a LaB6 filament, a lattice resolution of 0.25 nm and an acceleration voltage of 200 kV. HRTEM micrographs were taken at random locations across the grids, to ensure a non-biased assessment. Samples were prepared by drop-casting a few microliters of dispersion onto holey carbon films (copper grids) and dried at 120 ºC under vacuum for 12 hours. A water dispersion of GO (0.2 mg/mL) was employed to carried out dynamic light scattering (DLS, Malvern 4700 with goniometer and 7132 correlator, with an argon-ion laser operating at 488 nm; the measurements were made at the scattering angle of 90°). Also, in order to analyze the stability of the GO dispersion the absorbance at 660 nm [44] was recorded, during 5 hours of dispersions (0.2 mg/mL of GO in water, saline solution and in Luria Broth medium) using a Hewlett-Packard 8453 diode array UV–visible spectrophotometer.

**2.3. Bacterial Culture.**

*P. aeruginosa* (strain ATCC 15692 / PAO1) was used as strain models in this study. The bacterial strains were streaked and grown overnight under aerobic conditions (16 h) at 37 °C in Luria Broth (LB) agar plates from frozen stock. One colony of each strain was inoculated in 20 mL LB medium overnight at 37 °C with shaking. This culture was used as a source for the experiments and it was statically incubated and reduced to a final density of $1x10^6$ CFU/mL (colony-forming units per milliliter) determined by comparing the $OD_{600}$ of the sample with a standard curve relating $OD_{600}$ to cell number.

**2.4. Antibacterial activity in the dark**

Bacteria were cultured overnight in LB broth at 37 °C with shaking. An aliquot of the bacterial culture was aseptically transferred to fresh broth and incubated at 37 ºC to the exponential growth phase, where the bacterial concentration of the suspension was $10^6$ CFU/mL in saline solution (0.85% NaCl). The Gram-negative cells were incubated with GO over a wide range of concentrations. The bacteria were inoculated into Eppendorf and incubated for 3 h with GO at 37 °C. Bacterial cells (*P. aeruginosa*, $10^6$ CFU/mL) were inoculated in saline solutions containing different concentrations of GO (2, 6, 13, 20, 40, 60, 80, 100 and 120 μg/mL).

A bactericidal effect is defined as a decrease in the cell concentration (CFU/mL) after 24 h. Colonies were counted and compared with those on control plates to calculate changes in cell-growth inhibition. In the control test, the cells were treated with an isotonic saline solution without GO. Negative controls consisting of a bacteria-free medium were used. The percentage of bacterial growth inhibition was calculated using the difference between numbers of colonies from bacteria cultivated in presence of GO dispersions and those from bacteria as control. All treatments were prepared in triplicate and repeated in three independent experiments.

**2.5. Photothermal antibacterial activity of GO**

Bacterial cells ($10^6$ CFU/mL) were inoculated in a saline solution containing 2 μg/mL GO during 3 h, and were subsequently treated by NIR laser irradiation (875 nm, 500 mW) for 15 minutes. Afterwards, the cells were incubated for 5 h at 37 °C in LB medium. The dark control group was performed under the same experimental procedure but without for laser irradiation. The light control group was performed under the same experimental procedures but without the incorporation of GO. Finally, the percentage of bacterial growth inhibition

post-treatment was calculated using the difference between the numbers of colonies from bacteria incubated with GO respect to those from bacteria in the control. All treatments were prepared in triplicate and repeated in three independent experiments.

### 2.6. Viability Test

Bacterial cells were stained with a LIVE/DEAD® BacLight™ Bacterial Viability Kit (Life Technologies, Carlsbad, CA, USA), whereby live cells are stained green with SYTO 9 and dead cells are stained red with propidium iodide (PI). The *P. aeruginosa* cells were exposed to different treatments; i. Control group: cells without GO nor NIR exposure, ii. Light Control group: cells without GO exposed to NIR, iii. Dark Control group: cells with GO not exposed to NIR, and iv. GO+Light group: cells with GO and exposed to NIR for 24 h at 37 °C. Afterwards, the culture medium was removed and the samples were rinsed with saline solution, stained with LIVE/DEAD BacLight™ for 15 min in the dark. Cells were finally examined by fluorescence microscopy (Nikon Eclipse 50i). The light microscopy system was additionally equipped with filters to acquire epifluorescence images of the live (green fluorescent) and dead (red fluorescent) cells.

### 2.7. DNA fragmentation

*P. aeruginosa* cells were grown in LB medium, washed with saline solution, and re-suspended in saline solution at a concentration of $1\times10^8$ CFU/mL.

The cells were exposed to four different treatments; i. Control group: cells incubated 3h without GO nor NIR exposure, ii. Light Control group: cells incubated without GO exposed for 15 min to NIR irradiation, iii. Dark Control group: cells incubated with 5 μg/mL of GO not exposed to NIR, and iv. GO+Light group: cells incubated with 5 μg/mL with GO and

exposed to NIR for 15 min of NIR irradiation. After 5 hours, genomic DNA was isolated using a Genomic DNA Isolation Kit (Accuprep® Genomic DNA Extraction Kit, Bioneer trade (Shanghai) Co., Ltd) and DNA fragmentation was evaluated by agarose gel electrophoresis. The DNA electrophoresis of the four samples and DNA molecular weight marker was performed in 1% agarose gel containing 1 mg/mL gel green and migrated for 90 min at 80 V, and the DNA fragments were visualized by exposing the gel to light, followed by photography.

### 2.8. Statistical analysis

The results were CFU/mL and analyzed by one-way analysis of variance (ANOVA) followed by post hoc statistical tests, using the Tukey test for each pair of compared groups. Statistical significance was defined as $p<0.05$.

## 3. Results and Discussion

### 3.1. Graphene oxide characterization

One of the advantages of using GO instead of graphene lies in its easy dispersion in aqueous solutions, which is very important for bio-applications. The GO prepared in this study is highly dispersible in water, as it can be seen in the digital photography (**Figure 1A)** of a typical GO dispersion (2 mg/mL). In addition, the absorbance at 660 nm of GO dispersions (in water, saline solution and LB medium) remains almost constant during 5 hours (**Fig. 1A**) suggesting good stability as no precipitation of solid GO occurs in this period of time. This ensures dispersion stability during the experiments or applications. The spectroscopic characterization of the GO utilized is shown in **Fig. 1B-D**. The FTIR spectrum presents several bands that can be attributed to the presence of diverse types of oxygen functionalities

such as C=O carbonyl stretching centered at 1721 $cm^{-1}$; C–OH stretching at 1220 $cm^{-1}$, and C-O stretching at ~1038 $cm^{-1}$. Moreover, the O–H deformation vibration at 1390 $cm^{-1}$, and the O-H stretching vibrations at 3400 $cm^{-1}$ are clearly observed. Also, the C=C vibration mode from graphitic domains that have not been oxidized appears at 1600 $cm^{-1}$ (**Fig. 1B**) [45].

The Raman spectrum of GO is shown in **Fig. 1C** where the characteristic bands associated with D and G modes can be observed at 1350 $cm^{-1}$ and 1610 $cm^{-1}$, respectively [46]. Additionally, the Raman spectrum shows that the G band is broadened and shifted to 1594 $cm^{-1}$ in comparison with the starting graphite, which is an indication of the diminution of the size of in-plane $sp^2$ domains due to the exhaustive oxidation [47]. Moreover, the relationship between the intensity of D and G band (ID/IG ratio), a parameter commonly used to evaluate the oxidation degree of graphene-like materials [48], gives a value of around 0.8 resembling that of very oxidized materials [49]. The ID/IG ratio is associated to the size of the $sp^2$ domains it has been demonstrated that it increases with oxidation degree [50,51]. Pulido *et al.*, show that an ID/IG ratio of 0.8 corresponds to a C/O ratio of 1.8 obtained from the curve fitting of XPS spectra [52]. Therefore, we can assume a high degree of oxygenated moieties, responsible for the good stability of GO dispersions.

Two UV-visible bands characteristic of GO: the first, a shoulder at c.a. 300 nm, corresponding to n-π* transition of the C=O groups [53] and the other, which appears at 230 nm that is attributed to a π-π* plasmonic peak is shown in **Fig. 1D** [54]. All the spectroscopies, Raman, FTIR, and UV-visible, verify that the synthesized materials correspond to graphene with a reasonable oxidation degree.

The size of GO is a very important parameter that can strongly affect its biocompatibility, although there is not a consensus about the impact of GO lateral size and their effects in vitro [35,55]. The dimensions of the dispersed GO flakes were analyzed by HRTEM. The **Fig. 1E** shows a representative image of GO deposited onto TEM grids from water dispersions, where small laminates very well distributed can be observed. Statistical analysis (of at least 40 flakes) reveals that the average length and width of the flakes are around 350 ± 98 nm and 225 ± 50 nm, respectively, in agreement with lateral dimensions of GO prepared under similar conditions [56]. The size of GO laminates determined by HRTEM was also confirmed by DLS experiment (**Fig. 1F**) that reveals a GO mean size of 437.6 nm.

### 3.2. Antibacterial activity in the dark

To investigate the antibacterial activity of the GO against *P. aeruginosa* bacteria, the colony forming count (CFU) method was employed. In this study, the antibacterial viability was evaluated by analyzing the cell viability of the *P. aeruginosa* incubated during 3h in saline solution with different concentrations of GO at 37 °C. It is possible to observe in **Fig. 2** that as the GO concentrations increased the *P. aeruginosa* viability exponentially decreases. Based on these results, the antimicrobial activity of the GO dispersions increased in a dose-dependent manner. Moreover, 120 μg/mL of GO almost completely killed the *P. aeruginosa* bacteria (0.042 % of viability) incubated in a saline solution. The results show that when 120 μg/mL GO dispersed in the saline solution is employed, the growth of Gram-negative bacteria is almost completely suppressed. Therefore, the GO dispersions at this concentration could be used as a potent antibacterial agent. In summary, GO dispersion shows the excellent antibacterial function to Gram-negative bacteria. These results are comparable with recent

reports describing the strong antibacterial activity of Chlorin e6 molecule loaded on polyethylene glycol (PEG)-functionalized graphene [57].

### 3.3. Photothermal destruction of bacterial cell

The photothermal killing of the bacterial cells was tested using a continuous wave solid-statelaser of 785 nm wavelength, with a fluence of 500 mW/cm$^2$, as the excitation light source and 2 μg/mL of GO dispersion.

This concentration was chosen due to in the cell viability test showed negligible diminution on the *P. aeruginosa* viability. Moreover, many research studies have confirmed that GO in this concentration presents a good biocompatibility regardless of the size, time and cell type dependent cytotoxicity [58]. For instance Zhang *et al.* detected that the cytotoxicity in HeLa cells was only detected with GO dispersion of 20 μg/ mL, besides a lot of cell floating were observed after incubating the cell with 40 μg/mL of GO dispersion for 24 h [59]. In adenocarcinomic human alveolar basal epithelial (A549) cells, nor obvious effects on the morphology, viability, mortality, and membrane integrity were observed incubating the cell with GO at concentration of 10 μg/mL[55]. Also, in BEAS-2B (human lung cells) significant decreases in cell viability were observed at concentrations of 10-100 μg/mL [60]. The HBI.F3 (human neural stem cell line) cell viability was decreased with increasing GO concentration form 25 to 200 μg/mL [61]. As well, GO concentrations of 142 μg/mL leads 50 % lysis of Human Erythrocytes [62] and GO acting on human fibroblast cells exerts toxicity at doses greater than 50 μg/mL [63].

The bacteria cell viability was assessed by the plate-count technique. The means and standard deviations of the CFU/mL obtained for the studied groups after treatments are shown in **Fig. 3**.

Based on these results, the photoelimination of *P. aeruginosa* (GO+Light) were statistically significant, compared with the other groups: Control, Dark Control and Light Control (**Fig. 3**). As it can be seen, Light Control and Dark Control do not present any bactericidal effect on *P. aeruginosa*. Insignificant reduction of colonies was observed in the dark, suggesting that this bacteria strain is not affected by GO at a concentration of 2 μg/mL without external stimulus. Under NIR laser irradiation (Light Control), the bacteria survival rate is high in the absence of photothermal agents, indicating that the NIR laser alone is harmless to the bacterial strain. On the other hand, the NIR light and GO interaction exhibits a very high bactericidal activity after 5 h treatment. In addition, the results suggest that the large decrease in viability caused by local heating is accompanied by complete disintegration of the bacteria. Therefore, the combination of GO and NIR light irradiation, used in this study for a specific bacterium, represents an interesting tool to destroy pathogens.

In this work, the reduction between two different test Control and others (Light Control, Dark Control, and GO+Light) is quantified using the bacterial reduction ratio (LAR) following **Equation 1** [64].

$$LAR = \log\left[\frac{(CFU/mL)_{control}}{(CFU/\mathrm{mL})_{others}}\right] \quad (1)$$

Where (CFU/mL) control is the bacteria colony forming unit value per milliliter on control test, (CFU/mL) others is the bacteria colony forming unit value per milliliter in the other

conditions (Light Control, Dark Control, GO+Light). Also, the bacterial growth reduction percentage (%Rad) between the control and the other treatments is expressed in percentage and was calculated using **Equation 2.**

$$\%R_{ad} = (1 - 10^{-LAR})x\ 100 \qquad \textbf{(2)}$$

Where $10^{-LAR}$ is equal to the ratio between (CFU/mL) others to (CFU/mL) control; and $(1 - 10^{-LAR}) = \left(\frac{(CFU/\mathrm{mL})_{control} - (CFU/mL)_{others}}{(CFU/\mathrm{mL})_{control}}\right)$; that represents the normalized reduction of the number of colonies between the control and the other treatments.

The CFU/mL, Log CFU/mL, LAR, and % Rad values obtained in the test are depicted in **Table 1.**

It is possible to observe that the percentage reduction in bacterial growth obtained in the Dark Control (6.89 %) and Light Control (8.62 %) experiments are insignificant compared with the Control (0%). These results indicate that the 2 μg/mL GO dispersion exhibits no change in the percentage viability *per se*. Further, a high %Rad value obtained when the NIR light interacts with the GO (98.49 %) indicates that the decrease in the percentage of cell viability is clearly due to the GO photothermal effect. It is well known that a good antibacterial compound should selectively target bacteria over mammalian cells [59], and the combination of GO with laser irradiation at 785 nm could pave the way. The benefit of GO over other photothermal agents used for the ablation of pathogens is associated with the low laser power

used, making the approach more attractive. This hyperthermia approach might, potentially, become a new adjuvant therapeutic method for bacterial infections.

### 3.4. Viability Test

To verify the reliability of the CFU method, fluorescence microscopy was used to further examine the survival rate of cells after 15 min photothermal treatment with 2 μg/mL of GO dispersion. The live and dead bacterial cells tests were subsequently conducted to visually check the cell integrity disruption and bactericidal effect of the various treatments carried out. As shown in **Fig. 4A**, in the control experiment few dead cells were found. In Figure 4B, for the group treated without NIR irradiation (Dark Control), only very few *P. aeruginosa* are stained by PI suggesting that GO in dark condition is not enough to induce cell death. Also, same results were observed for cells irradiated in absence of GO (Light Control) (**Fig. 4C**). However, in the case of the group treated with GO and irradiated with NIR laser (GO+Light), the most of bacteria are stained by PI (**Fig. 4D**), indicating that this treatment produces damage in the cells. This observation suggests that GO can efficiently induce cell death by disrupting the cellular membrane integrity triggered by hyperthermia. The effective killing of bacteria lies in the photothermal effect, whereby GO absorbs radiation and subsequently releases that energy as heat to its closely surrounding environment. The heating suddenly increases the local temperature, which triggers damage to different macromolecules such as proteins and lipids in the cell membrane, and finally, leads to bacterial death. The results are in agreement with those reported by Khan *et al.*[65] and Tian *et al.*[66] that demonstrated the synergistic effect of combining GO and a 1064 nm Nd-YAG laser for antibacterial and antifungal treatments.

### 3.5. DNA fragmentation

The amount of DNA from untreated and treated *P. aeruginosa* cells was evaluated by agarose gel electrophoresis. Agarose gel electrophoresis of the isolated DNA from *P. aeruginosa* Control and Light Control not exhibit DNA fragmentation (**Fig. 5**), while isolated DNA cultivated with GO (5 μg/mL) presents a slight fragmentation. On the contrary, the isolated DNA from *P. aeruginosa* treated with GO and irradiated exhibits a clear DNA fragmentation (**Fig. 5**). This photothermal antibacterial effect could be attributed to membrane stress induced by GO and NIR irradiation, which may result in physical damage to cell membranes, leading the loss of bacterial membrane integrity and DNA leakage. Further, our results suggest that the mechanism of antibacterial activity of GO depends on DNA fragmentation. It has been demonstrated by Kumar *et al*. that nanoparticles of ZnO and $TiO_2$ produce DNA damage and cell death in *E. coli*.[67] However, these nanomaterials induce cell death due to the toxicity of the nanoparticles, in contrast, our results demonstrate that GO dispersions do not exhibit noticeable DNA damage while that the combination of GO and a radiation trigger provokes damage to cell membranes, leading to the loss of bacterial membrane integrity and the leakage of DNA.

## 4. Conclusion

In this work, an unmodified GO dispersion showed significant antibacterial activity against pathogen microorganism such as *P. aeruginosa* in a concentration-dependent manner, demonstrating that the GO dispersions at high concentration could be used as a potent antibacterial agent. Dispersion of unmodified GO in a concentration of 120 μg/mL ensures 99.9 % mortality of the bacteria in the dark. Additionally, by applying NIR radiation on a low concentration of unmodified GO (2 μg/mL) a clear photothermal effect is observed with

a reduction of cell viability of 98.49 %. Using fluorescence microscopy, it is found that a low concentration of unmodified GO dispersions can efficiently induce cell death by NIR triggered hyperthermia which disrupts the integrity of the cell membrane. Moreover, clear DNA fragmentation is observed by electrophoresis. In summary, this study demonstrates the enormous potential of unmodified GO dispersion as an antibacterial agent both in the dark (high GO concentrations) and under NIR illumination (low GO concentrations). These results allow us to suggest a novel therapy for combating bacterial nosocomial infections that avoids the use of conventional drugs which nowadays are developing high bacterial resistance.

**Conflict of interest statement**

All the authors declare to have no conflict of interest.

**Acknowledgements**

This work was supported by FONCYT (PICT-2716-2013, the SUMA2 Network Project, 7th Framework Program of the European Commission (IRSES ProjectNr. 318903), enabling movability. C.A. Barbero D.F. Acevedo, E.I. Yslas are permanent research fellows of CONICET. J.Y. Pereyra thanks CONICET for graduate fellowships. The funding of FONCYT (PICT-2716-2013), CONICET, and SECYT-UNRC is gratefully acknowledged.

**References**

[1] S.J. McConoughey, R. Howlin, J.F. Granger, M.M. Manring, J.H. Calhoun, M. Shirtliff, S. Kathju, P. Stoodley, Biofilms in periprosthetic orthopedic infections., Future Microbiol. 9 (2014) 987–1007. doi:10.2217/fmb.14.64.

[2] S. Reardon, Antibiotic resistance sweeping developing world, Nat. News. 509 (2014) 141–142. doi:10.1038/509141a.

[3] P.S. Stewart, Mechanisms of antibiotic resistance in bacterial biofilms, Int. J. Med. Microbiol. 292 (2002) 107–113. doi:10.1078/1438-4221-00196.

[4] WHO, WHO's first global report on antibiotic resistance reveals serious, worldwide threat to public health, World Heal. Organ. (2014) News Release.

[5] C.L. Ventola, The antibiotic resistance crisis: part 1: causes and threats., P T A Peer-Reviewed J. Formul. Manag. 40 (2015) 277–83. doi:Article.

[6] M. Chatterjee, C.P. Anju, L. Biswas, V. Anil Kumar, C. Gopi Mohan, R. Biswas, Antibiotic resistance in Pseudomonas aeruginosa and alternative therapeutic options, Int. J. Med. Microbiol. 306 (2016) 48–58. doi:10.1016/j.ijmm.2015.11.004.

[7] A. Raghunath, E. Perumal, Metal oxide nanoparticles as antimicrobial agents: a promise for the future, Int. J. Antimicrob. Agents. 49 (2017) 137–152. doi:10.1016/j.ijantimicag.2016.11.011.

[8] W. Salem, D.R. Leitner, F.G. Zingl, G. Schratter, R. Prassl, W. Goessler, J. Reidl, S. Schild, Antibacterial activity of silver and zinc nanoparticles against Vibrio cholerae and enterotoxic Escherichia coli, Int. J. Med. Microbiol. 305 (2015) 85–95. doi:10.1016/j.ijmm.2014.11.005.

[9] N. Beyth, Y. Houri-Haddad, A. Domb, W. Khan, R. Hazan, Alternative antimicrobial approach: Nano-antimicrobial materials, Evidence-Based Complement. Altern. Med. 2015 (2015). doi:10.1155/2015/246012.

[10] W.-C. Huang, P.-J. Tsai, Y.-C. Chen, Multifunctional Fe3O4@Au nanoeggs as photothermal agents for selective killing of nosocomial and antibiotic-resistant bacteria., Small. 5 (2009) 51–6. doi:10.1002/smll.200801042.

[11] F. Zhou, D. Xing, Z. Ou, B. Wu, D.E. Resasco, W.R. Chen, Cancer photothermal therapy in the near-infrared region by using single-walled carbon nanotubes, J. Biomed. Opt. 14 (2009) 21007–21009.

[12] R. Weissleder, A clearer vision for in vivo imaging., Nat. Biotechnol. 19 (2001) 316–7. doi:10.1038/86684.

[13] N.J. Millenbaugh, J.B. Baskin, M.N. DeSilva, W.R. Elliott, R.D. Glickman, Photothermal killing of Staphylococcus aureus using antibody-targeted gold nanoparticles., Int. J. Nanomedicine. 10 (2015) 1953–60. doi:10.2147/IJN.S76150.

[14] J. Wu, J. Gao, Y. Xie, X. Chen, Photo-nano-therapy for bactericidal using graphene oxide, in: Prog. Biomed. Opt. Imaging - Proc. SPIE, 2015. doi:10.1117/12.2079438.

[15] W. Jo, M.J. Kim, Influence of the photothermal effect of a gold nanorod cluster on biofilm disinfection., Nanotechnology. 24 (2013) 195104. doi:10.1088/0957-4484/24/19/195104.

[16] C.-B. Kim, D.K. Yi, P.S.S. Kim, W. Lee, M.J. Kim, Rapid photothermal lysis of the pathogenic bacteria, Escherichia coli using synthesis of gold nanorods., J. Nanosci. Nanotechnol. 9 (2009) 2841–5. doi:10.1166/jnn.2009.002.

[17] A.H.. Castro Neto, N.M.R.. Peres, K.S.. Novoselov, A.K.. Geim, F. Guinea, The electronic properties of graphene, Rev. Mod. Phys. 81 (2009) 109–162. doi:10.1103/RevModPhys.81.109.

[18] K. Olszowska, J. Pang, P.S. Wrobel, L. Zhao, H.Q. Ta, Z. Liu, B. Trzebicka, A. Bachmatiuk, M.H. Rummeli, Three-dimensional nanostructured graphene: Synthesis and energy, environmental and biomedical applications, Synth. Met. 234 (2017) 53–85. doi:10.1016/j.synthmet.2017.10.014.

[19] K.S. Novoselov, A.K. Geim, S. V Morozov, D. Jiang, Y. Zhang, S. V Dubonos, I. V Grigorieva, A.A. Firsov, Electric field effect in atomically thin carbon films., Science. 306 (2004) 666–9. doi:10.1126/science.1102896.

[20] W. Gao, The chemistry of graphene oxide, in: Graphene Oxide Reduct. Recipes, Spectrosc. Appl., 2015: pp. 61–95. doi:10.1007/978-3-319-15500-5_3.

[21] S.Y. Wu, S.S.A. An, J. Hulme, Current applications of graphene oxide in nanomedicine, Int. J. Nanomedicine. 10 (2015) 9–24. doi:10.2147/IJN.S88285.

[22] B. Zhang, Y. Wang, G. Zhai, Biomedical applications of the graphene-based materials, Mater. Sci. Eng. C. 61 (2016) 953–964. doi:10.1016/j.msec.2015.12.073.

[23] J.Y. Pereyra, E.A. Cuello, R.C. Rodriguez, C.A. Barbero, E.I. Yslas, H.J. Salavagione, D.F. Acevedo, Synthesis and characterization of GO-hydrogels composites, in: IOP Conf. Ser. Mater. Sci. Eng., 2017. doi:10.1088/1757-899X/258/1/012002.

[24] A. Gallardo, Y. Pereyra, E. Martínez-Campos, C. García, D. Acitores, I. Casado-Losada, M.A. Gómez-Fatou, H. Reinecke, G. Ellis, D. Acevedo, J. Rodríguez-Hernández, H.J. Salavagione, Facile one-pot exfoliation and integration of 2D layered materials by dispersion in a photocurable polymer precursor, Nanoscale. 9 (2017). doi:10.1039/c7nr03204h.

[25] O. Akhavan, E. Ghaderi, Toxicity of graphene and graphene oxide nanowalls against bacteria, ACS Nano. 4 (2010) 5731–5736. doi:10.1021/nn101390x.

[26] A.F. de Faria, D.S. Martinez, S.M. Meira, A.C. de Moraes, A. Brandelli, A.G. Filho, O.L. Alves, Anti-adhesion and antibacterial activity of silver nanoparticles supported on graphene oxide sheets, Colloids and surfaces.B, Biointerfaces. 113 (2014) 115–124.

[27] P. De Marco, S. Zara, M. De Colli, M. Radunovic, V. Lazović, V. Ettorre, A. Di Crescenzo, A. Piattelli, A. Cataldi, A. Fontana, Graphene oxide improves the biocompatibility of collagen membranes in an in vitro model of human primary gingival fibroblasts, Biomed. Mater. 12 (2017). doi:10.1088/1748-605X/aa7907.

[28] I.M. Martinez Paino, F. Santos, V. Zucolotto, Biocompatibility and toxicology effects of graphene oxide in cancer, normal, and primary immune cells, J. Biomed. Mater. Res. - Part A. 105 (2017) 728–736. doi:10.1002/jbm.a.35946.

[29] O.N. Ruiz, K.A.S. Fernando, B. Wang, N.A. Brown, P.G. Luo, N.D. McNamara, M. Vangsness, Y.P. Sun, C.E. Bunker, Graphene oxide: a nonspecific enhancer of cellular growth, ACS Nano. 5 (2011) 8100–8107. doi:10.1021/nn202699t.

[30] M. Wojtoniszak, X. Chen, R.J. Kalenczuk, A. Wajda, J. Łapczuk, M. Kurzewski, M. Drozdzik, P.K. Chu, E. Borowiak-Palen, Synthesis, dispersion, and cytocompatibility of graphene oxide and reduced graphene oxide, Colloids Surfaces B Biointerfaces. 89 (2012) 79–85. doi:10.1016/j.colsurfb.2011.08.026.

[31] A. Sasidharan, L.S. Panchakarla, P. Chandran, D. Menon, S. Nair, C.N.R. Rao, M. Koyakutty, Differential nano-bio interactions and toxicity effects of pristine versus

functionalized graphene, Nanoscale. 3 (2011) 2461–2464. doi:10.1039/c1nr10172b.

[32] J.H. Liu, T. Wang, H. Wang, Y. Gu, Y. Xu, H. Tang, G. Jia, Y. Liu, Biocompatibility of graphene oxide intravenously administrated in mice - Effects of dose, size and exposure protocols, Toxicol. Res. (Camb). 4 (2014) 83–91. doi:10.1039/c4tx00044g.

[33] K. Yang, J. Wan, S. Zhang, B. Tian, Y. Zhang, Z. Liu, The influence of surface chemistry and size of nanoscale graphene oxide on photothermal therapy of cancer using ultra-low laser power., Biomaterials. 33 (2012) 2206–14. doi:10.1016/j.biomaterials.2011.11.064.

[34] V. Gies, S. Zou, Systematic toxicity investigation of graphene oxide: Evaluation of assay selection, cell type, exposure period and flake size, Toxicol. Res. (Camb). 7 (2018) 93–101. doi:10.1039/c7tx00278e.

[35] H. Yue, W. Wei, Z. Yue, B. Wang, N. Luo, Y. Gao, D. Ma, G. Ma, Z. Su, The role of the lateral dimension of graphene oxide in the regulation of cellular responses, Biomaterials. 33 (2012) 4013–4021. doi:10.1016/j.biomaterials.2012.02.021.

[36] E.L.K. Chng, M. Pumera, The toxicity of graphene oxides: Dependence on the oxidative methods used, Chem. - A Eur. J. 19 (2013) 8227–8235. doi:10.1002/chem.201300824.

[37] X. Zhang, J. Yin, C. Peng, W. Hu, Z. Zhu, W. Li, C. Fan, Q. Huang, Distribution and biocompatibility studies of graphene oxide in mice after intravenous administration, Carbon N. Y. 49 (2011) 986–995. doi:10.1016/j.carbon.2010.11.005.

[38] Y.A. Cheon, J.H. Bae, B.G. Chung, Reduced Graphene Oxide Nanosheet for

Chemo-photothermal Therapy, Langmuir. 32 (2016) 2731–2736. doi:10.1021/acs.langmuir.6b00315.

[39] X. Jia, I. Ahmad, R. Yang, C. Wang, Versatile graphene-based photothermal nanocomposites for effectively capturing and killing bacteria, and for destroying bacterial biofilms, J. Mater. Chem. B. 5 (2017) 2459–2467. doi:10.1039/C6TB03084J.

[40] J. Kim, L.J. Cote, F. Kim, W. Yuan, K.R. Shull, J. Huang, Graphene oxide sheets at interfaces, J. Am. Chem. Soc. 132 (2010) 8180–8186. doi:10.1021/ja102777p.

[41] M.C. Wu, A.R. Deokar, J.H. Liao, P.Y. Shih, Y.C. Ling, Graphene-based photothermal agent for rapid and effective killing of bacteria, ACS Nano. 7 (2013) 1281–1290. doi:10.1021/nn304782d.

[42] A. Jarosz, M. Skoda, I. Dudek, D. Szukiewicz, Oxidative Stress and Mitochondrial Activation as the Main Mechanisms Underlying Graphene Toxicity against Human Cancer Cells, Oxid. Med. Cell. Longev. 2016 (2016) 1–14. doi:10.1155/2016/5851035.

[43] W.S. Hummers, R.E. Offeman, Preparation of Graphitic Oxide, J. Am. Chem. Soc. 80 (1958) 1339–1339. doi:10.1021/ja01539a017.

[44] D. Konios, M.M. Stylianakis, E. Stratakis, E. Kymakis, Dispersion behaviour of graphene oxide and reduced graphene oxide, J. Colloid Interface Sci. 430 (2014) 108–112. doi:10.1016/j.jcis.2014.05.033.

[45] F. Cataldo, Structural Analogies and Differences Between Graphite Oxide and $C_{60}$ and $C_{70}$ Polymeric Oxides (Fullerene Ozopolymers), Fullerenes, Nanotub. Carbon

Nanostructures. 11 (2003) 1–13. doi:10.1081/FST-120018670.

[46] K.N. Kudin, B. Ozbas, H.C. Schniepp, R.K. Prud'homme, I.A. Aksay, R. Car, Raman spectra of graphite oxide and functionalized graphene sheets, Nano Lett. 8 (2008) 36–41. doi:10.1021/nl071822y.

[47] A.C. Ferrari, J.C. Meyer, V. Scardaci, C. Casiraghi, M. Lazzeri, F. Mauri, S. Piscanec, D. Jiang, K.S. Novoselov, S. Roth, A.K. Geim, Raman spectrum of graphene and graphene layers, Phys. Rev. Lett. 97 (2006). doi:10.1103/PhysRevLett.97.187401.

[48] G.K. Ramesha, S. Sampath, Electrochemical Reduction of Oriented Graphene Oxide Films: An in Situ Raman Spectroelectrochemical Study, J. Phys. Chem. C. 113 (2009) 7985–7989. doi:10.1021/jp811377n.

[49] S.-G. Kim, O.-K. Park, J.H. Lee, B.-C. Ku, Layer-by-layer assembled graphene oxide films and barrier properties of thermally reduced graphene oxide membranes, Carbon Lett. 14 (2013) 247–250. doi:10.5714/CL.2013.14.4.247.

[50] D. Torres, J.L. Pinilla, R. Moliner, I. Suelves, On the oxidation degree of few-layer graphene oxide sheets obtained from chemically oxidized multiwall carbon nanotubes, Carbon N. Y. 81 (2015) 405–417. doi:10.1016/j.carbon.2014.09.073.

[51] M. Pelin, L. Fusco, V. León, C. Martín, A. Criado, S. Sosa, E. Vázquez, A. Tubaro, M. Prato, Differential cytotoxic effects of graphene and graphene oxide on skin keratinocytes, Sci. Rep. 7 (2017). doi:10.1038/srep40572.

[52] A. Pulido, P. Concepción, M. Boronat, C. Botas, P. Alvarez, R. Menendez, A. Corma, Reconstruction of the carbon sp2 network in graphene oxide by low-

temperature reaction with CO, J. Mater. Chem. 22 (2012) 51–56. doi:10.1039/c1jm14514b.

[53] P. Khanra, T. Kuila, N.H. Kim, S.H. Bae, D. sheng Yu, J.H. Lee, Simultaneous bio-functionalization and reduction of graphene oxide by baker's yeast, Chem. Eng. J. 183 (2012) 526–533. doi:10.1016/j.cej.2011.12.075.

[54] T. Kuila, P. Khanra, S. Bose, N.H. Kim, B.-C. Ku, B. Moon, J.H. Lee, Preparation of water-dispersible graphene by facile surface modification of graphite oxide, Nanotechnology. 22 (2011) 305710. doi:10.1088/0957-4484/22/30/305710.

[55] Y. Chang, S.-T. Yang, J.-H. Liu, E. Dong, Y. Wang, A. Cao, Y. Liu, H. Wang, In vitro toxicity evaluation of graphene oxide on A549 cells, Toxicol. Lett. 200 (2011) 201–210. doi:10.1016/j.toxlet.2010.11.016.

[56] V.P. and A.B. Julie Russier, Emanuele Treossi, Alessia Scarsi, Francesco Perrozzi, Hélène Dumortier, Luca Ottaviano, Moreno Meneghetti, Evidencing the mask effect of graphene oxide: a comparative study on primary human and murine phagocytic cells., Biomaterials. 7 (2013) 11234–47. doi:10.1016/j.addr.2013.07.006.

[57] S. Liu, T.H. Zeng, M. Hofmann, E. Burcombe, J. Wei, R. Jiang, J. Kong, Y. Chen, Antibacterial activity of graphite, graphite oxide, graphene oxide, and reduced graphene oxide: Membrane and oxidative stress, ACS Nano. 5 (2011) 6971–6980. doi:10.1021/nn202451x.

[58] X. Guo, N. Mei, Assessment of the toxic potential of graphene family nanomaterials, J. Food Drug Anal. 22 (2014) 105–115. doi:10.1016/j.jfda.2014.01.009.

[59] X. Zhang, W. Hu, J. Li, L. Tao, Y. Wei, A comparative study of cellular uptake and

cytotoxicity of multi-walled carbon nanotubes, graphene oxide, and nanodiamond, Toxicol. Res. (Camb). 1 (2012) 62. doi:10.1039/c2tx20006f.

[60] N.V.S. Vallabani, S. Mittal, R.K. Shukla, A.K. Pandey, S.R. Dhakate, R. Pasricha, A. Dhawan, Toxicity of graphene in normal human lung cells (BEAS-2B), J. Biomed. Nanotechnol. 7 (2011) 106–107. doi:10.1166/jbn.2011.1224.

[61] S.-M. Kang, T.-H. Kim, J.-W. Choi, Cell Chip to Detect Effects of Graphene Oxide Nanopellet on Human Neural Stem Cell, J. Nanosci. Nanotechnol. 12 (2012) 5185–5190. doi:10.1166/jnn.2012.6378.

[62] K.-H. Liao, Y.-S. Lin, C.W. Macosko, C.L. Haynes, Cytotoxicity of graphene oxide and graphene in human erythrocytes and skin fibroblasts., ACS Appl. Mater. Interfaces. 3 (2011) 2607–15. doi:10.1021/am200428v.

[63] K. Wang, J. Ruan, H. Song, J. Zhang, Y. Wo, S. Guo, D. Cui, Biocompatibility of Graphene Oxide, Nanoscale Res. Lett. 6 (2011) 1–8. doi:10.1007/s11671-010-9751-6.

[64] L.A. Gallarato, L.E. Mulko, M.S. Dardanelli, C.A. Barbero, D.F. Acevedo, E.I. Yslas, Synergistic effect of polyaniline coverage and surface microstructure on the inhibition of Pseudomonas aeruginosa biofilm formation, Colloids Surfaces B Biointerfaces. 150 (2017). doi:10.1016/j.colsurfb.2016.11.014.

[65] M. Shahnawaz Khan, H.N. Abdelhamid, H.F. Wu, Near infrared (NIR) laser mediated surface activation of graphene oxide nanoflakes for efficient antibacterial, antifungal and wound healing treatment, Colloids Surfaces B Biointerfaces. 127 (2015) 281–291. doi:10.1016/j.colsurfb.2014.12.049.

[66] B. Tian, C. Wang, S. Zhang, L. Feng, Z. Liu, Photothermally enhanced photodynamic therapy delivered by nano-graphene oxide., ACS Nano. 5 (2011) 7000–9. doi:10.1021/nn201560b.

[67] A. Kumar, A.K. Pandey, S.S. Singh, R. Shanker, A. Dhawan, Engineered ZnO and TiO(2) nanoparticles induce oxidative stress and DNA damage leading to reduced viability of Escherichia coli., Free Radic. Biol. Med. 51 (2011) 1872–81. doi:10.1016/j.freeradbiomed.2011.08.025.

**Figure captions**

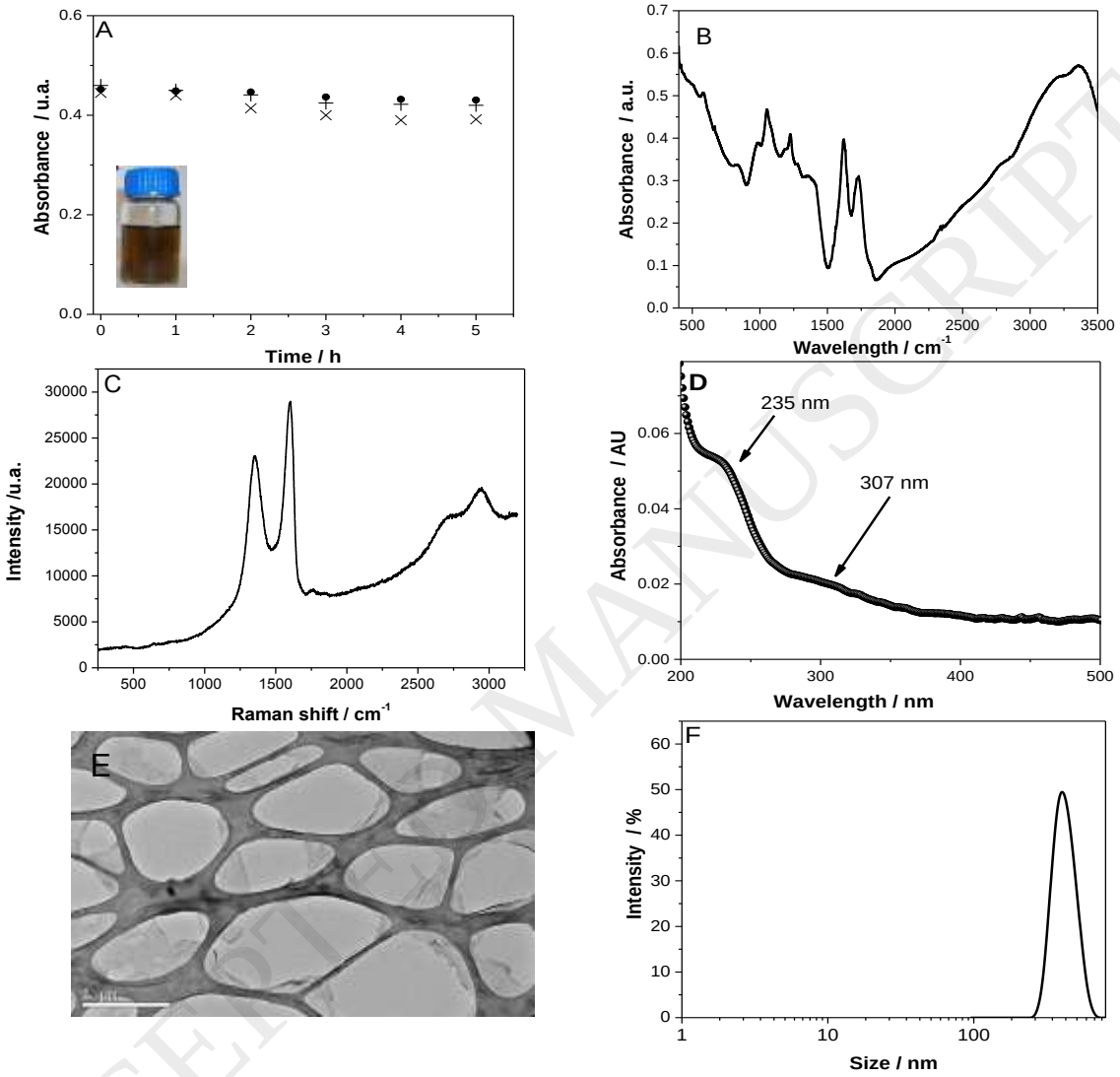


**Fig. 1.** Photography of an aqueous dispersion of GO (2 mg/mL) and absorbance at 660 nm of GO (0.2 mg/mL) in: water (•), saline solution (+) and LB medium (x) versus time (A), Characterization of the GO employed in this study by: FTIR spectroscopy (B), Raman spectroscopy (C), UV-visible spectroscopy (D), High-resolution transmission electron microscopy (E), and Dynamic light scattering (F).

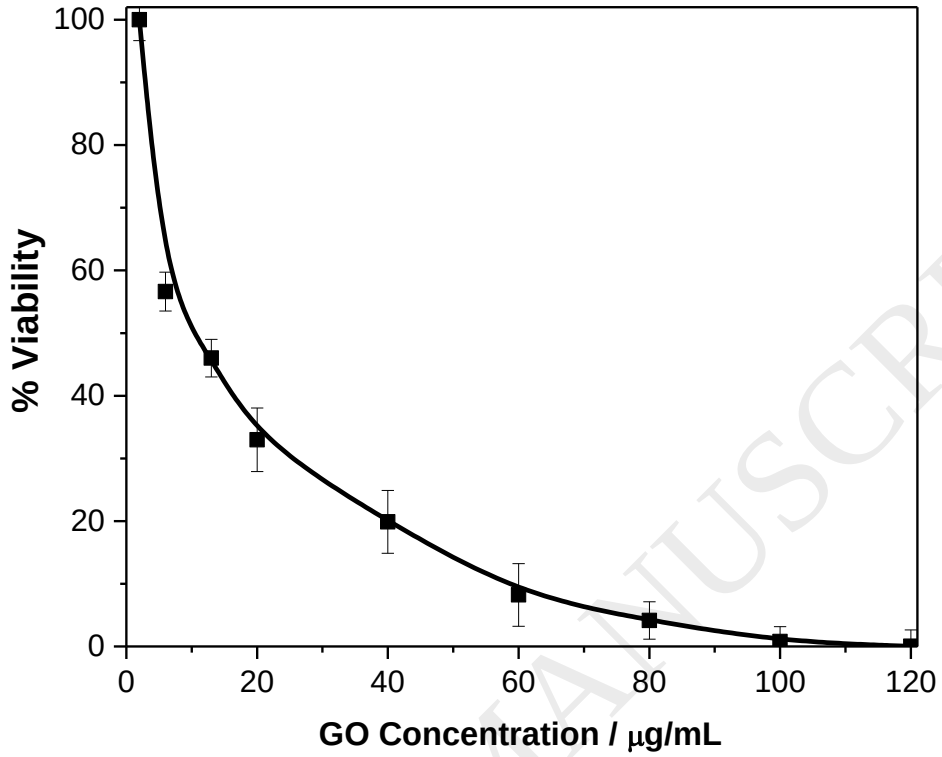


**Fig. 2.** Cell viability percentage after incubation with GO dispersions. Different concentrations of GO were incubated with *P. aeruginosa* ($10^6$ CFU/mL), at 37 °C for 3 h. Loss of cell viability rates was obtained by colony counting method. Error bars represent the standard deviation.

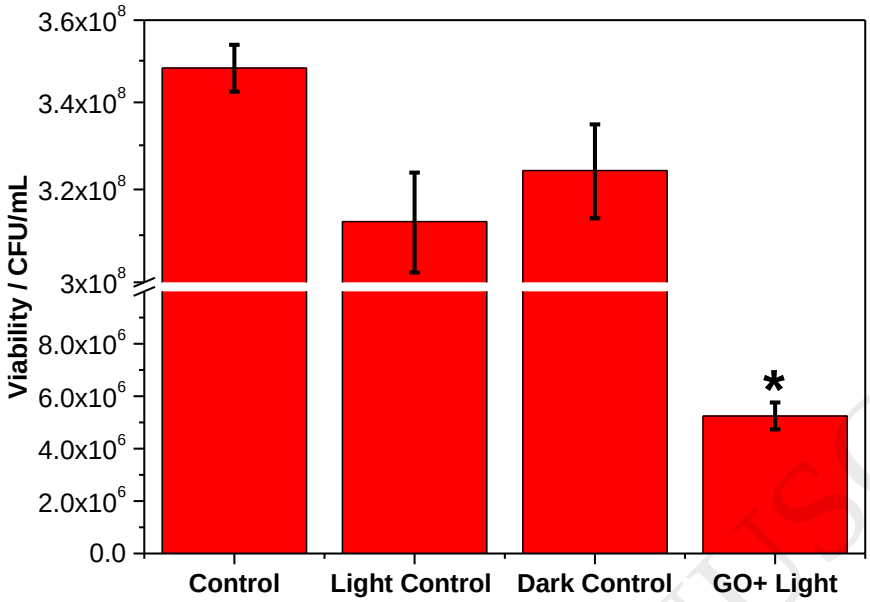


**Fig. 3.** Effect of different treatment on *P. aeruginosa* cell viability. Data are shown as means and standard deviations calculated from three independent experiment. The treated group (GO+Light) showed statistically significant differences from the control group by analysis of variance (ANOVA) followed by post hoc statistical tests, using the Tukey test (*$p < 0.05$).

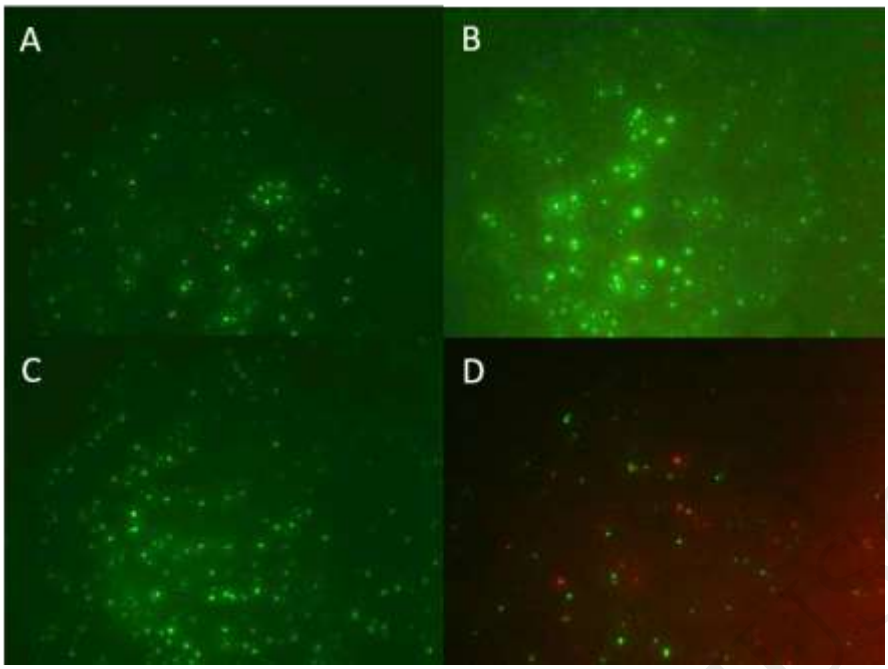


**Fig. 4:** Fluorescence images of live (green) and dead (red) bacterial cells of *P. aeruginosa* of A) Control cells B) Light Control C) Dark Control and D) GO+Light. Samples were stained and evaluated after staining them with LIVE/DEAD BacLight$^{TM}$ Bacterial Viability Kit. Live bacteria appear as green, dead bacteria as red.

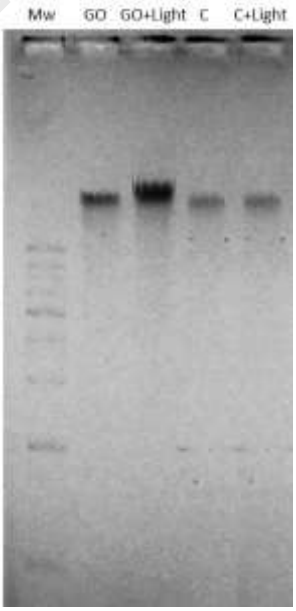

**Fig. 5.** Agarose gel electrophoresis of DNA lane 1 (Mw): molecular weight marker, lane 2 (GO): *P. aeruginosa* after treatment with GO, lane 3 (GO+Light): *P. aeruginosa* with GO after irradiation with NIR laser, lane 4 (C): *P. aeruginosa* Control and lane 5 (C+Light): *P. aeruginosa* after irradiation with NIR laser.

**Table**

**Table 1:** Viable bacterial cells quantity grown before the laser irradiation (CFU/mL), bacterial reduction ratio (LAR), reduction percentage (% $R_{ad}$)

| | CFU/mL ($x10^{-8}$) | Log CFU/mL | LAR | % $R_{ad}$ |
|---|---|---|---|---|
| Control | 3.48 | 8.54 | 0 | 0 |
| Light Control | 3.13 | 8.50 | 0.039 | 8.62 |
| Dark Control | 3.24 | 8.51 | 0.03 | 6.89 |
| GO+Light | 0.05 | 6.71 | 1.82 | 98.49 |